ISBN: 978-3-95450-248-6 ISSN: 2673-5490 doi: 10.18429/JACoW-IPAC2025-TUPM077

NEW DEVELOPMENTS IN THE DESIGN OF THE MUON PRODUCTION TARGET AREA OF A MULTI-TeV MUON COLLIDER*

J. Mańczak†, C. Ahdida, L. Bottura, S. Candido, M. Calviani, D. Calzolari, R. F. Ximenes, A. Lechner, G. Lerner, D. Schulte, CERN, Geneva, Switzerland
C. Rogers, ISIS Neutron and Muon Source, STFC, Oxfordshire, United Kingdom
A. Portone, Fusion for Energy, Barcelona, Spain

Abstract

As the International Muon Collider Collaboration advances the conceptual design for a multi-TeV muon collider facility, new technical constraints continue to arise in the muon production stage, where a high-power proton beam interacts with a target. Achieving the required muon bunch intensity may necessitate increasing the primary beam power up to 4 MW. Consequently, the shielding design must address sustained radiation exposure, particularly on critical components such as superconducting solenoids, which generate strong magnetic fields essential for capturing pions and decay muons. This study presents the latest results from FLUKA Monte Carlo simulations, modelling the radiation load on solenoids, and comparing different target materials.

INTRODUCTION

The International Muon Collider Collaboration (IMCC) is studying the feasibility of a multi-TeV muon collider facility [1–6]. One of the key technical challenges lies in the muon production, which involves directing a high-power proton beam onto a target. This process generates secondary pions, which are captured by high-field solenoids and subsequently decay into muons. The IMCC is working on an integrated front-end design that incorporates effective engineering solutions to generate the required high-intensity, high-brightness muon beam.

One of the options considered for the proton beam parameters include a proton energy of 10 GeV and a beam power of 4 MW, representing a significant increase compared to the previously studied baseline case of 5 GeV and 2 MW beam [7]. This escalation in beam energy and power introduces additional challenges for shielding optimization, as the higher-energy interactions result in more intense secondary particle showers and increased radiation loads on critical components. The baseline target assembly consists of an 80 cm-long isostatic graphite rod (density: 1.7 g/cm^3 with a 30 mm diameter), enclosed in a titanium vessel filled with helium gas [8]. However, the previously considered static helium design was found not adequate for the increased proton beam power. Instead, the current proposed solution relies on a helium vessel with forced convection to enhance heat dissipation and prevent excessive temperatures in the target.

Table 1: Proton Driver Beam Parameters

Beam power [MW]	4	Pulse frequency [Hz]	5
Beam energy [GeV]	10	Beam size $\sigma_{x,y}$ [mm]	5
Protons per pulse		$5 \cdot 10^{14}$	

A liquid lead target is being investigated as an alternative, to benefit from its high thermal power absorption capacity and resistance to radiation damage when dealing with the increased proton beam power [9]. Another option under consideration is fluidized tungsten. Given the MW-scale power, substantial radiation shielding is necessary in the target region to protect the equipment. The solenoids near the target are also subjected to secondary particle showers produced by inelastic proton collisions in the target. To mitigate these effects, radiation absorbers must be installed within the magnet aperture to reduce the shower intensity before reaching the coils. The shielding serves multiple purposes: preventing beam-induced magnet quenches, limiting thermal load on the cryogenic system, and protecting magnets from cumulative radiation damage. The latter includes ionizing dose effects on organic materials (such as insulation and spacers) and atomic displacements in superconductors. Similar radiation studies have been conducted for muon production front-ends in previous projects, including neutrino factories and the US-Muon Accelerator Program (MAP) [10–13].

Building on the IMCC's efforts, this paper presents studies on power deposition and radiation damage in the proposed target and front-end design for the updated primary beam parameters shown in Table 1 (unless mentioned otherwise). The increase in beam energy and intensity requires a reassessment of shielding strategies to protect critical components, particularly the newly developed pion-capture solenoid, which employs high-temperature superconductors (HTS) without normal-conducting inserts and achieves a peak magnetic field of 20 T. We evaluate the necessary shielding configurations to safeguard the HTS magnets and analyze the impact of the target material on the muon yield and cumulative radiation load. All simulations were conducted using the FLUKA Monte Carlo code [14–16].

FRONT-END LAYOUT

The FLUKA simulation geometry employed for assessing muon yield and radiation exposure to equipment is illustrated in Fig. 1. This streamlined model is an extension of the geometry described in [7]. The front-end consists of a sequence of high-temperature superconducting (HTS) solenoids with uniform apertures, spanning a total length

* Funded by the European Union (EU). Views and opinions expressed are however those of the author(s) only and do not necessarily reflect those of the EU or European Research Executive Agency (REA). Neither the EU nor the REA can be held responsible for them.
† jerzy.mikolaj.manczak@cern.ch

ISBN: 978-3-95450-248-6 ISSN: 2673-5490 doi: 10.18429/JACoW-IPAC2025-TUPM077

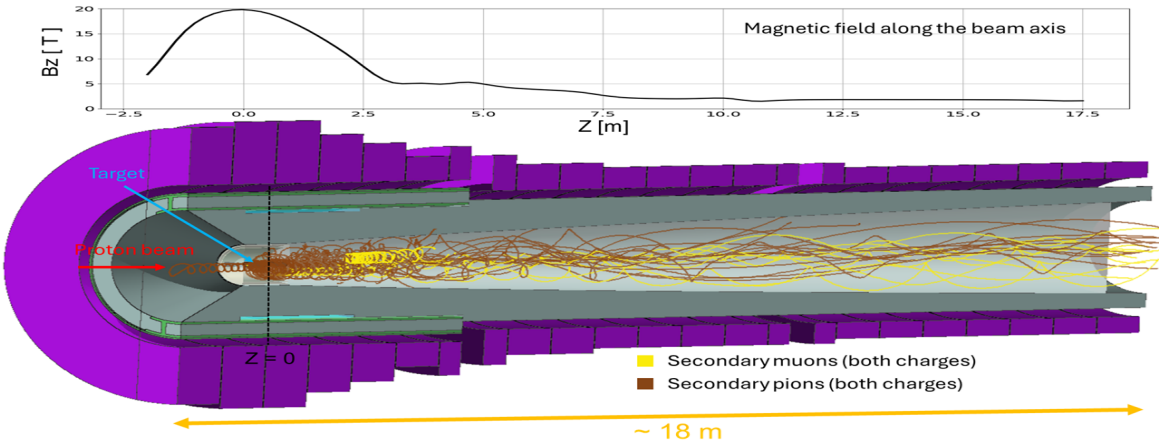

Figure 1: FLUKA model used for radiation studies. The structural beams are depicted in green and the HTS magnets are purple. The blue stripes close to the target represent the neutron-mitigating layer. As was concluded from earlier studies [7], the shielding can be reduced further downstream from the target and the neutron-mitigating layer is no longer necessary past the seventh coil. The example secondary muon and pion tracks are visualized for 20 primary proton events.

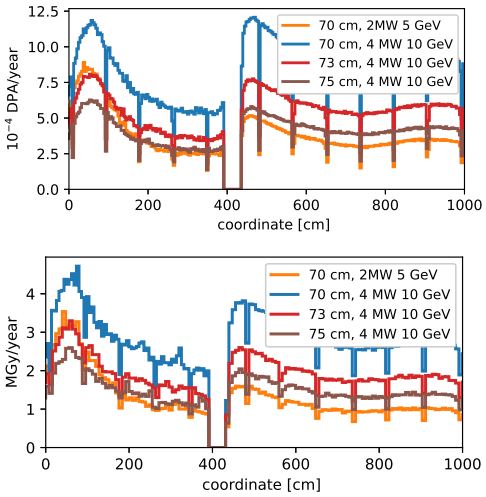

Figure 2: Maximum ionizing dose and DPA per year along the HTS target solenoids for various magnet bore sizes and proton beam parameters. The labels give the inner radius of the magnets in the vicinity of the target. The graphite target extends from 40 cm to 120 cm in the Z-coordinate.

of approximately 18 meters. These solenoids incorporate radiation shielding composed of tungsten segments, some of which are cooled using helium gas. There are two 48 cm gaps between cryostats left for structural elements. Two support beams are passing through the shielding volume to preliminarily account for the integration constraints. Their presence forces the neutron-mitigating layer, described in [7], to be placed closer to the target, which effectively reduces its efficiency. The magnetic field strength gradually decreases from 20 T at the target to 1.5 T at the end of the tapered region. The solenoid arrangement remains an active area of optimization, and the configuration presented here is primarily designed to establish the desired magnetic field distribution and have a first verification of the engineering and integration. The vessel corresponds to the scenario with the static graphite target. In the case of liquid lead, the vessel is removed and the lead target is placed in vacuum, without accounting yet for a lead-flow system equipment. The FLUKA simulations explored various shielding thicknesses, ranging from approximately 43 cm to 48 cm.

Aside from the baseline graphite rod target, two liquid lead geometries were analysed: a lead curtain, modelled as a rectangular lead block with dimensions of 30x16x1.5 cm, and a lead rod, serving as a simplified representation of a lead jet system. The dimensions of the lead curtain were selected to fully contain the primary beam while accounting for engineering constraints. The lead rod, with a length of 28 cm and a radius of 0.52 cm, was dimensioned by scaling the original graphite target according to the ratio of the proton inelastic scattering lengths in the two materials (16 cm in lead and 48 cm in graphite). In the simulations of lead rod configuration, the proton beam size, $\sigma_{x,y}$, was reduced to approximately 0.175 mm to match the rescaled transverse size of the rod. The described lead rod geometry is not considered a technically viable option, but it is used to quantify the impact of the target material while removing dependency on the target shape.

CUMULATIVE RADIATION DAMAGE IN HTS SOLENOIDS

Currently, the goal of the shielding design is to keep the maximum displacement damage and the absorbed dose in the HTS coils at the level of 10^{-3} DPA/year and 5 MGy/year. These limits, especially the one on DPA, are indicative, and may need to be revised once the research on radiation damage in HTS advances.

Figure 2 shows the maximum ionizing dose and DPA in the HTS coils along the beam direction with the primary beam energy of 10 GeV and 4 MW of power for different maximum coil apertures and the baseline graphite target scenario. The results are given for one operational year, assuming a run time of 1.2×10^7 s (equivalent to ≈140 days

ISBN: 978-3-95450-248-6 ISSN: 2673-5490 doi: 10.18429/JACoW-IPAC2025-TUPM077

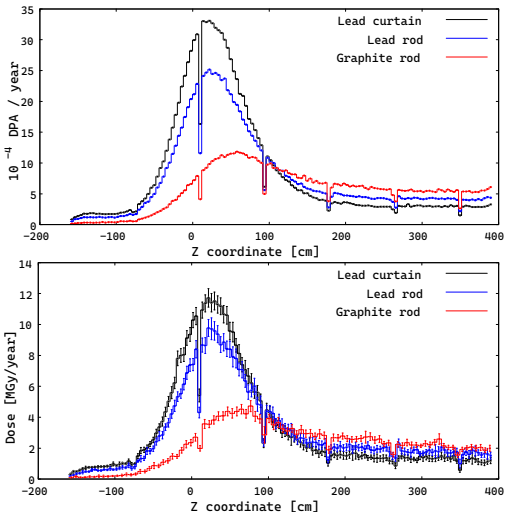

Figure 3: Maximum ionizing dose and DPA per year along the HTS target solenoids. See text for description.

with 100% machine availability). The DPA calculation is based on the Norget-Torrens-Robinson (NRT)-model [17] in FLUKA, with the material-specific damage threshold energies taken from Ref. [18]. The second peak present at z around 450 cm is due to the shielding becoming smaller and the neutron-absorbing layer no longer being present. The reduction in the radiation damage with the increasing aperture is not only due to thicker shielding, but also to the position of the neutron-mitigating layer whose distance from the structural beam is kept constant in the simulation. The studies indicate that the magnet bore size would have to be increased by 3 cm to arrive at peak radiation damage levels comparable to the 2 MW, 5 GeV proton beam case. With a 4 MW beam, a shielding thickness of about 46 cm (inner magnet radius of 73 cm) results in a peak dose of about 3 MGy/year, and a displacement damage of about $0.8 \cdot 10^{-3}$ DPA/year.

Graphite vs Liquid Lead

Figure 3 shows the maximum DPA and ionizing dose in the HTS for different target options. The shielding configuration corresponds to the baseline case indicated as "70 cm" in Fig. 2. For both geometries, liquid lead generates a significantly higher radiation load than graphite, peaking at $3 \cdot 10^{-3}$ DPA/year and ~12 MGy/year. Due to longitudinal re-scaling, the number of primary interactions remains similar between all the target options, but in the case of lead the interactions are condensed over a shorter distance, leading to more intense localized particle flux.

MUON YIELD

Figure 4 shows the muon and pion yields at the end of the tapering region for three different target options: graphite rod, lead rod and lead curtain. The momentum cut is based on the assumed acceptance of the subsequent bunching system. The lead rod produces roughly 10% more pions and positive muons and almost 40% more negative muons per

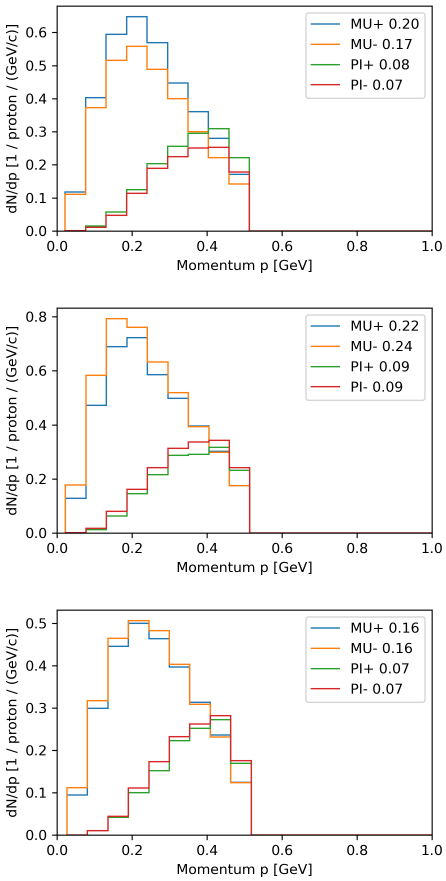

Figure 4: Muon and pion yield with a $p < 500$ MeV/c momentum cut at the end of the tapering for the graphite target (top), liquid lead rod (middle) and liquid lead curtain (bottom). The numbers in the legend correspond to the pion/muon yield per primary proton.

primary proton than the baseline graphite case. The curtain introduces a vertical barrier for the secondary particles produced in the target volume, as it can intercept their spiral trajectory in the solenoid field.

CONCLUSION

The paper compared three target options, consisting of a graphite rod, a lead rod-like option, and a lead curtain, in a proton-driven 4 MW target facility of a muon collider. Different aspects were investigated, focusing on the shielding requirements for protecting HTS solenoids and the muon yield at the end of the tapering region. Liquid lead is found to generally induce higher peak radiation load due to its shorter proton interaction length. At the same time, with carefully optimized geometry, liquid lead target can improve the muon yield generated by a 10 GeV proton beam with respect to the baseline graphite option. Instead, the lead curtain is found to cause a reduction of the muon and pion yield compared to the rod-shaped options. These results represent relevant input to the broader IMCC design studies of the target facility.

ISBN: 978-3-95450-248-6 ISSN: 2673-5490 doi: 10.18429/JACoW-IPAC2025-TUPM077

REFERENCES

[1] D. Schulte, "The International Muon Collider Collaboration", in *Proc. IPAC'21*, Campinas, Brazil, May 2021, pp. 3792–3795. doi:10.18429/JACoW-IPAC2021-THPAB017

[2] D. Schulte, "The Muon Collider", in *Proc. IPAC'22*, Bangkok, Thailand, 2022, pp. 821–826. doi:10.18429/JACoW-IPAC2022-TUIZSP2

[3] C. Accettura *et al.*, "Towards a muon collider", *Eur. Phys. J. C*, vol. 83, no. 9, p. 864, 2023. doi:10.1140/epjc/s10052-023-11889-x

[4] C. Accettura *et al.*, "Interim report for the International Muon Collider Collaboration (IMCC)", CERN, Geneva, Switzerland, Rep. CERN-2024-002, 2024. doi:10.23731/CYRM-2024-002

[5] C. Accettura *et al.*, "MuCol Milestone Report No. 5: Preliminary Parameters", *Zenodo*, Nov. 2024. doi:10.5281/zenodo.13970100

[6] C. Accettura *et al.*, "The Muon Collider", Fermi National Accelerator Laboratory, Illinois, USA, Rep. FERMILAB-PUB-25-0309-AD-PPD-T, Apr. 2025.

[7] J. Manczak *et al.*, "Radiation load studies for the proton target area of a multi-TeV muon collider", no. 15, pp. 2544–2547, Jul. 2024. doi:10.18429/JACoW-IPAC2024-WEPR28

[8] F. J. S. Esteban *et al.*, "Muon Collider Graphite Target Studies and Demonstrator Layout Possibilities at CERN", in *Proc. IPAC'22*, Bangkok, Thailand, 2022, pp. 2895–2898. doi:10.18429/JACoW-IPAC2022-THPOTK052

[9] S. Candido *et al.*, "Magnetohydrodynamic effects in liquid lead target concept for a muon collider", presented at IPAC'25, Taipei, Taiwan, Jun. 2025, paper THPB017, this conference.

[10] N. V. Mokhov, "Particle Production and Radiation Environment at a Neutrino Factory Target Station", in *Proc. PAC'01*, Chicago, IL, USA, Jun. 2001, paper FOAC010, pp. 745–747. https://jacow.org/p01/papers/FOAC010.pdf

[11] J. J. Back *et al.*, "Particle Production Simulations for the Neutrino Factory Target", in *Proc. IPAC'11*, San Sebastian, Spain, 2011, paper MOPZ008, pp. 835–837. https://jacow.org/IPAC2011/papers/MOPZ008.pdf

[12] J. J. Back, C. Densham, R. Edgecock, and G. Prior, "Particle production and energy deposition studies for the neutrino factory target station", *Phys. Rev. ST Accel. Beams*, vol. 16, no. 2, p. 021001, Feb. 2013. doi:10.1103/PhysRevSTAB.16.021001

[13] H. G. Kirk *et al.*, "Beam-power Deposition in a 4-MW Target Station for a Muon Collider or a Neutrino Factory", in *Proc. IPAC'11*, San Sebastian, Spain, 2011, paper TUPS054, pp. 1653–1655. https://jacow.org/IPAC2011/papers/TUPS054.pdf

[14] CERN, Fluka website. https://fluka.cern

[15] G. Battistoni, T. Boehlen, F. Cerutti, P. W. Chin, L. S. Esposito, A. Fassò, *et al.*, "Overview of the FLUKA code", *Ann. Nucl. Energy*, vol. 82, pp. 10–18, 2015. doi:10.1016/j.anucene.2014.11.007

[16] C. Ahdida, D. Bozzato, D. Calzolari, F. Cerutti, N. Charitonidis, A. Cimmino, *et al.*, "New Capabilities of the FLUKA Multi-Purpose Code", *Front. Phys.*, vol. 9, 2022. doi:10.3389/fphy.2021.788253

[17] MJ. Norgett, MT. Robinson, and IM. Torrens, "A proposed method of calculating displacement dose rates", *Nucl. Eng. Des.*, vol. 33, no. 1, pp. 50–54, 1975. doi:10.1016/0029-5493(75)90035-7

[18] RE. MacFarlane and AC. Kahler, "Methods for Processing ENDF/B-VII with NJOY", *Nucl. Data Sheets*, vol. 111, no. 12, pp. 2739–2890, 2010. doi:10.1016/j.nds.2010.11.001